

Cite this: *RSC Adv.*, 2019, 9, 26757Received 14th June 2019  
Accepted 19th August 2019

DOI: 10.1039/c9ra04481g

rsc.li/rsc-advances

# Lipid-lowering and antioxidative effects of *Apium graveolens* L. root flavonoid extracts†

Yuan He,<sup>a</sup> Yang Shi,<sup>b</sup> Airong Zhang,<sup>a</sup> Xiaoxia Zhang,<sup>a</sup> Jing Sun<sup>a</sup> and Li Tian<sup>\*,a</sup>

Flavonoids are the major components of *Apium graveolens* L. root (AR). In this study, we used a rat model of high-fat emulsion diet induced hyperlipidemia (HLP) to examine the antioxidant and lipid-lowering effects of the AR flavonoid extract (ARFE), and to identify its potential targets by molecular docking and western-blotting. ARFE significantly lowered the serum lipid levels in HLP rats. The lipid-lowering targets of ARFE were predicted and validated, which showed that ARFE significantly downregulated the expression levels of cholesterol synthesis-associated target proteins, including SREBP1, HMGCR and ACC1. These findings demonstrate that ARFE has remarkable lipid-lowering and antioxidant effects, and the former is mediated by the inhibition of SREBP1, HMGCR and ACC1.

## 1. Introduction

Hyperlipidemia (HLP) is a common illness characterized by a high level of lipids in the blood, a result of abnormal elevation in total cholesterol (TC), triglycerides (TG) and low-density lipoprotein cholesterol (LDL-C) content, and reduction in high-density lipoprotein cholesterol (HDL-C). HLP is the direct cause of coronary heart disease,<sup>1</sup> arteriosclerosis,<sup>2</sup> acute pancreatitis,<sup>3</sup> cirrhosis,<sup>4</sup> gallstones,<sup>5</sup> peripheral vascular diseases,<sup>6</sup> hyperuricemia,<sup>7</sup> hypertension and diabetes.<sup>8–10</sup> In addition, the high levels of TC, TG and LDL-C in the HLP patients result in disorders of lipid metabolism, one of the major causes of oxidative stress wherein the rate of production of reactive oxygen species (ROS) exceeds their clearance rate. Since the liver is both the main source and target of ROS, HLP is also a key inducer of non-alcoholic fatty liver disease (NAFLD).<sup>11</sup>

Although fibrates and statins have been shown to be effective against HLP, they are limited by the irreversible side-effects that occur during long-term use. Therefore, recent efforts have focused on finding safer, natural alternatives for the treatment of HLP.<sup>12</sup> Previous studies have shown that *Apium graveolens* L., commonly known as celery, has potent antioxidant,<sup>13</sup> anti-spasmodic,<sup>14</sup> antihyperlipidemic<sup>15</sup> and hypotensive<sup>16</sup> effects. The dry root of *A. graveolens* L. is an edible herbal medicine, although its therapeutic effects have been less well-studied. *A. graveolens* L. root (AR) contains numerous bioactive components, including flavonoids, terpenes, sesquiterpenes, benzoquinones, phenols, sugars and tannins.<sup>17–19</sup> Our previous study

showed that the AR flavonoid extract (ARFE) lowered the serum lipid levels in HLP rats, although its dose–response relationship and mechanism of action remained unclear.

Molecular docking is a simulation technique that matches two or more molecules by space and energy. AutoDock Vina<sup>20</sup> is a widely used molecular docking software that identifies the mode of binding between small molecule receptors and proteins using a Lamarckian genetic algorithm, along with a search engine, and can calculate and compare the binding free energy to determine the probability of binding. The aim of this study was to determine the therapeutic effect and anti-HLP mechanism of ARFE in high-fat emulsion diet induced HLP rats, and to identify the targets of ARFE using the above approach.

## 2. Materials and methods

### 2.1 Chemical products and reagents

Three batches of AR were purchased from Hetian, Xinjiang (Lot no. 20170907, 20170910, 20170913). All specimens were stored in the Traditional Chinese Medicine Ethnical Herbs Specimen Museum of Xinjiang Medical University (Specimen no. 2017092001). The plant materials were identified by WULI-ya ShaYi-ti, a professor of Chinese medicine identification and research in the Xinjiang Medical University. Apigenin and apigenin-7-*O*- $\beta$ -D-glucopyranoside were purchased from Goybio Co. Ltd. (Shanghai, China), Apiin from Nanjing Goren Bio-Technology Co. Ltd. (Nanjing, China), and 3'-methoxyapiin from Nanjing SenBeijia Biotechnology Co. Ltd. (Nanjing, China). Xuezhikang capsule and lipanthyl micronised capsule were respectively purchased from Beijing Peking University WBL Biotech Co. Ltd. (Beijing, China) and Recipharm Fontaine (Fontaine-lès-Dijon, France). Kits for detecting superoxide dismutase (SOD) (no. 20180918), malondialdehyde (MDA) (no. 20180916) and glutathione peroxidase (GSH-Px) (no. 20180917) were

<sup>a</sup>College of Traditional Chinese Medicine, Xinjiang Medical University, Urumqi, Xinjiang, China. E-mail: tianli109@126.com

<sup>b</sup>Department of Editor, Xinjiang Medical University, Urumqi, Xinjiang, China

† Electronic supplementary information (ESI) available. See DOI: 10.1039/c9ra04481g



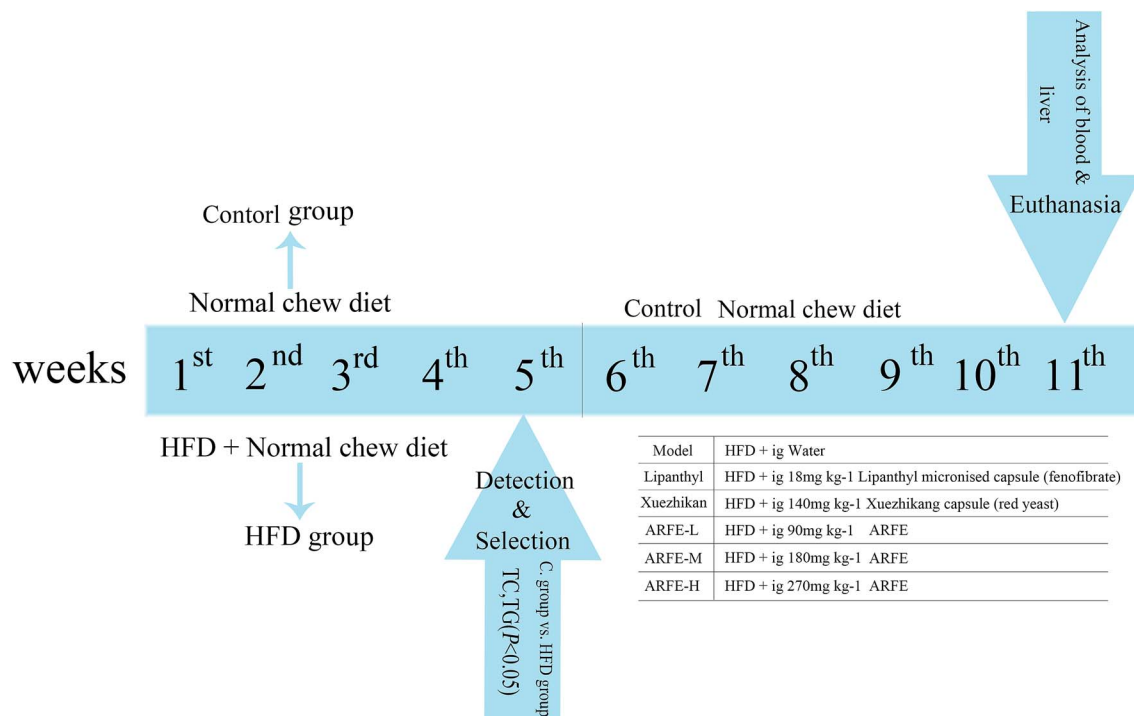


Fig. 1 Experimental design for ARFE treatment in HLP rats. Ig, intragastric gavage.

purchased from Nanjing Jiancheng Bioengineering Institute (Nanjing, China). BCA protein assay kit (RK240545) was purchased from Thermo Fisher Scientific (Waltham, MA, USA). Anti-sterol

regulatory element-binding protein 1 (SREBP1), anti-farnesyl-diphosphate farnesyltransferase 1 (FDFT1), and anti-HMG-CoA reductase (HMGCR) antibodies were purchased from Abcam

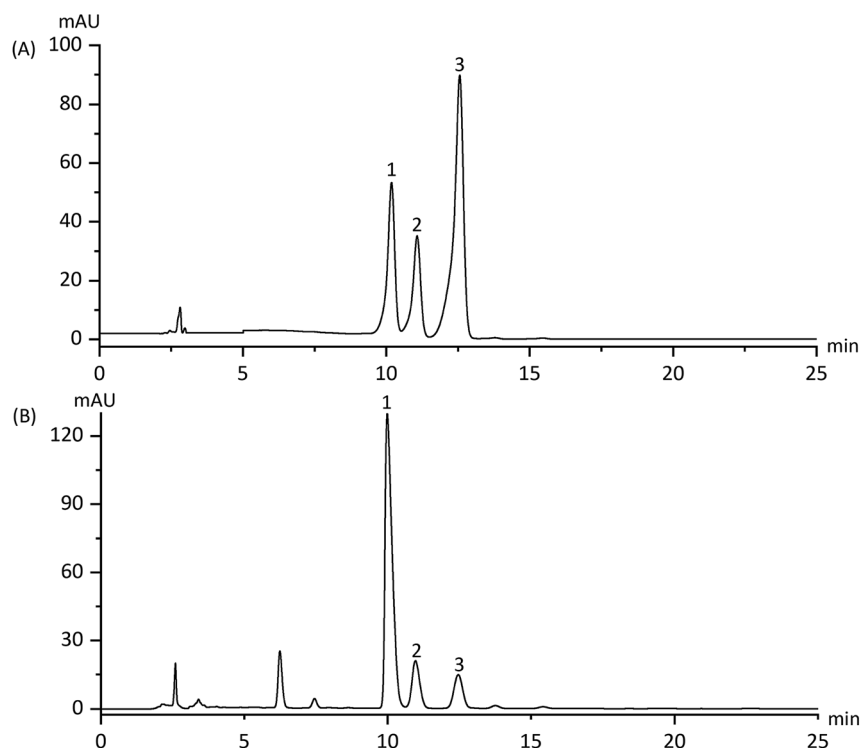


Fig. 2 HPLC spectra of the reference products (A) and ARFE (B). Peaks: (1) apiin; (2) 3'-methoxyapiin; (3) apigenin-7-O- $\beta$ -D-glucopyranoside.

Table 1 Apiin, 3'-methoxyapiin and apigenin-7-O-β-D-glucopyranoside content in ARFE

Peak no.	Assigned identity	Retention time (min)	Contents in ARFE (mg g <sup>-1</sup> )
1	Apiin	9.98	187.31
2	3'-Methoxyapiin	10.96	45.5
3	Apigenin-7-O-β-D-glucopyranoside	12.45	12.44

Shanghai Trading Co. Ltd. (Shanghai, China), the anti-acetyl-CoA carboxylase 1 (ACC1) antibody from Proteintech (Rosemont, IL, USA), and the anti-GAPDH and secondary antibodies from Elabscience Biotechnology Co. Ltd. (Wuhan, China). Other chemical products and reagents were of the highest grade commercially available.

## 2.2 Preparation of ARFE

AR powder was extracted twice by reflux (1 h each time) using 70% ethanol (1 : 6), and both extracts were combined and concentrated. The ethanol extract was then dissolved in distilled water and the pH was adjusted to 8. The solution was passed through D101 macroporous resins and eluted by 30% and 50% ethanol to obtain ARFE. The latter was quantitated by high performance liquid chromatography (HPLC, Agilent 1220) using acetonitrile and 0.1% phosphoric acid (21 : 79) as the mobile phase at the flow rate of 1 mL min<sup>-1</sup>, column temperature 25 °C and wavelength 340 nm.

## 2.3 Preparation of high-fat dairy

Using an optimized modification of a previously reported method,<sup>21</sup> 30 g melted lard, 10 g cholesterol and 1 g propylthiouracil were added to a 100 mL beaker and mixed with 6 mL Tween-80 to obtain the oil phase. In addition, 50 mL distilled water was poured into a 100 mL beaker, heated to 60 °C, and mixed with 10 g sucrose and 5 g sodium cholate to obtain the aqueous phase. The oil and aqueous phases were thoroughly mixed, and distilled water was added at 60 °C to obtain the high-fat dairy, which was eventually warmed at 45 °C in a water bath and vortexed prior to use.

## 2.4 Establishment of HLP model and treatment regimen

Eight-week-old Sprague Dawley rats (weigh 200 ± 20 g, equal number of females and males) were provided by the Experimental Animal Center of Xinjiang Medical University (Urumqi, China). All animals were housed in a specific pathogen-free (SPF) laboratory at 25 ± 1 °C, 60 ± 5% humidity and a 12 h/12 h light-dark cycle, with *ad libitum* access to food and water. All experiments were conducted in accordance with the "Guide for the Care and Use of Laboratory Animals" recommended by the National Institute of Health and approved by the Animal Ethics Committee of the First Affiliated Hospital of Xinjiang Medical University (Urumqi, China). After acclimatizing for one week, the animals were divided into the normal chow-fed control group, and the high-fat diet (HFD) group that received daily gavage of 10 mL kg<sup>-1</sup> high-fat emulsion for 5 consecutive weeks. At the end of the dietary regimen, the animals were fasted overnight, and their blood was collected from the fundal venous plexus to analyse serum lipid levels. The successfully modelled HLP rats with significantly higher (*P* < 0.05) serum TC and TG levels were randomly divided into 6 treatment groups (*n* = 8 per group) as outlined in Fig. 1. Lipanthyl micronised capsule (fenofibrate) and Xuezhikang capsule (red yeast)-fed rats were the positive controls. All rats had *ad libitum* access to water and food during the 11 week-long treatment regimen, following which the animals were fasted overnight and anesthetized. Blood was collected from the abdominal aorta and centrifuged, and the separated serum was stored at -80 °C. In addition, the liver lobules and aortic arches were also harvested, washed in saline and fixed in 10% formalin (pH 7.4) for 48 h. A portion of liver tissue was stored at -80 °C for subsequent biochemical analysis.

Table 2 Measurement of apiin, 3'-methoxyapiin and apigenin-7-O-β-D-glucopyranoside levels by HPLC – method validation<sup>a</sup>

Chemical	Calibration curve	Linearity		Precision RSD (%)	Repeatability RSD (%)	Recovery (%)	Limit of quantitation (μg mL <sup>-1</sup> )
		Correlation factor ( <i>r</i> <sup>2</sup> )	(mg mL <sup>-1</sup> )				
Apiin	$Y = 27\,365\,340.54x + 214\,217.29$	0.9998	0.24–0.84	0.14	0.11	98.7	10
3'-Methoxyapiin	$Y = 17\,026\,768.87x + 209\,822.11$	0.9997	0.26–0.91	0.12	0.65	98.29	15
Apigenin-7-O-β-D-glucopyranoside	$Y = 64\,779\,573.78x + 154\,434.71$	0.9998	0.22–0.77	0.1	1.02	97.69	6.5

<sup>a</sup> Samples were analyzed by HPLC, and standard curves were plotted to determine the concentration of each component. Results of 6 validation methods are expressed as mean values (*n* = 3), and the standard error of the mean (SEM) was <5%.

Table 3 Quality control data of the three batches of ARFE extracts

Batch	Contents in ARFE (mg g <sup>-1</sup> )			Average contents (mg g <sup>-1</sup> )		
	Apiin	3'-Methoxyapiin	Apigenin-7-O-β-D-glucopyranoside	Apiin	3'-Methoxyapiin	Apigenin-7-O-β-D-glucopyranoside
20170907	187.32	48.55	12.43	187.30	48.51	12.45
20170910	187.28	48.48	12.49			
20170913	187.31	48.50	12.44			

Table 4 Effect of ARFE on the rat body weight<sup>a</sup>

Group	Body weight (g)			
	Initial	5 weeks	7 weeks	11 weeks
Control	180 ± 4.2	323 ± 6.9	353 ± 3.1	461 ± 3.3
Model	180 ± 5.3	359 ± 6.6*	401 ± 5.2*	580 ± 9.4*
Xuezhikang	180 ± 4.1	364 ± 3.6*	404 ± 4.4*	501 ± 6.6*#
Lipanthyl	178 ± 6.5	356 ± 6.8*	398 ± 7.4*	524 ± 4.1*#
ARFE-L	180 ± 4.1	359 ± 5.4*	402 ± 6.3*	501 ± 4.3*#
ARFE-M	181 ± 3.2	353 ± 4.5*	399 ± 5.1*	504 ± 8.2*#
ARFE-H	179 ± 6.1	362 ± 3.6*	401 ± 4.8*	503 ± 5.2*#

<sup>a</sup> Body weight data is expressed as the mean ± SD of 8 animals per group. *P* < 0.05 indicates significant difference between two groups. \*, compare with Control group, #, compare with Model group.

## 2.5 Biochemical analysis

Serum TC, TG, LDL-C and HDL-C levels were measured using an automated biochemical analyser. The contents of SOD, MDA and GSH-Px in the liver tissue homogenates were measured using specific kits.

## 2.6 H&E staining

The formalin-fixed liver and aortic arch samples were dehydrated, embedded in paraffin, sectioned and stained with haematoxylin and eosin (H&E). The stained sections were examined under a microscope and photographed.

## 2.7 Molecular docking

The Therapeutic Target Database<sup>22</sup> and all relevant literature<sup>23–26</sup> were searched to identify HLP-associated targets as putative receptors for the drugs. The chemical structures of apigenin, apiin, 3'-methoxyapiin and apigenin-7-O-β-D-glucopyranoside were downloaded from The PubChem Project database and used as small molecule ligands. Molecular docking was performed using Autodock Vina, and the results were ordered by decreasing binding free energy. The building pocket parameters are shown in the Table 5. To increase reliability, the num-mode parameter was set to 20, the energy-range parameter to 5, and the exhaustivity value to 100. Correlation analysis was performed on the first 25 results.

## 2.8 Western blotting

Cytoplasmic proteins identified by molecular docking were validated by western blotting. Proteins were extracted using RIPA lysis buffer supplemented with 1% proteinase inhibitor, and quantified by the BCA protein assay kit. Equal amounts of protein per sample were separated by 8% SDS-PAGE, and transferred to a polyvinylidene fluoride film (PVDF; Indianapolis, IN, USA). The membranes were blocked with 5% skim milk for 1 h, and incubated overnight with the primary antibody at 4 °C. Following incubation with alkaline phosphatase-conjugated goat anti-rabbit secondary antibody for 1 h, the blots were developed with the substrate solution, and visualized using the Bio-Rad gel imaging system (Hercules, CA, USA). GAPDH was used as the loading control, and the relative protein levels were quantified using the Bio-Rad Image Lab software.

## 2.9 Statistical analysis

Data were analysed using GraphPad Prism v.8.0. All samples were measured in triplicates and the results are expressed as mean ± standard deviation (SD). The groups were compared using ANOVA, and *P* < 0.05 was considered statistically significant.

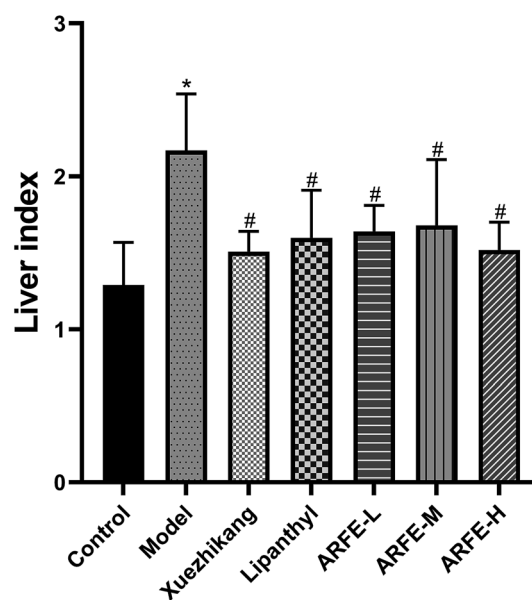


Fig. 3 Effect of ARFE on liver index of rats. *P* < 0.05 indicates significant difference between two groups. \*, compare with Control group, #, compare with Model group.

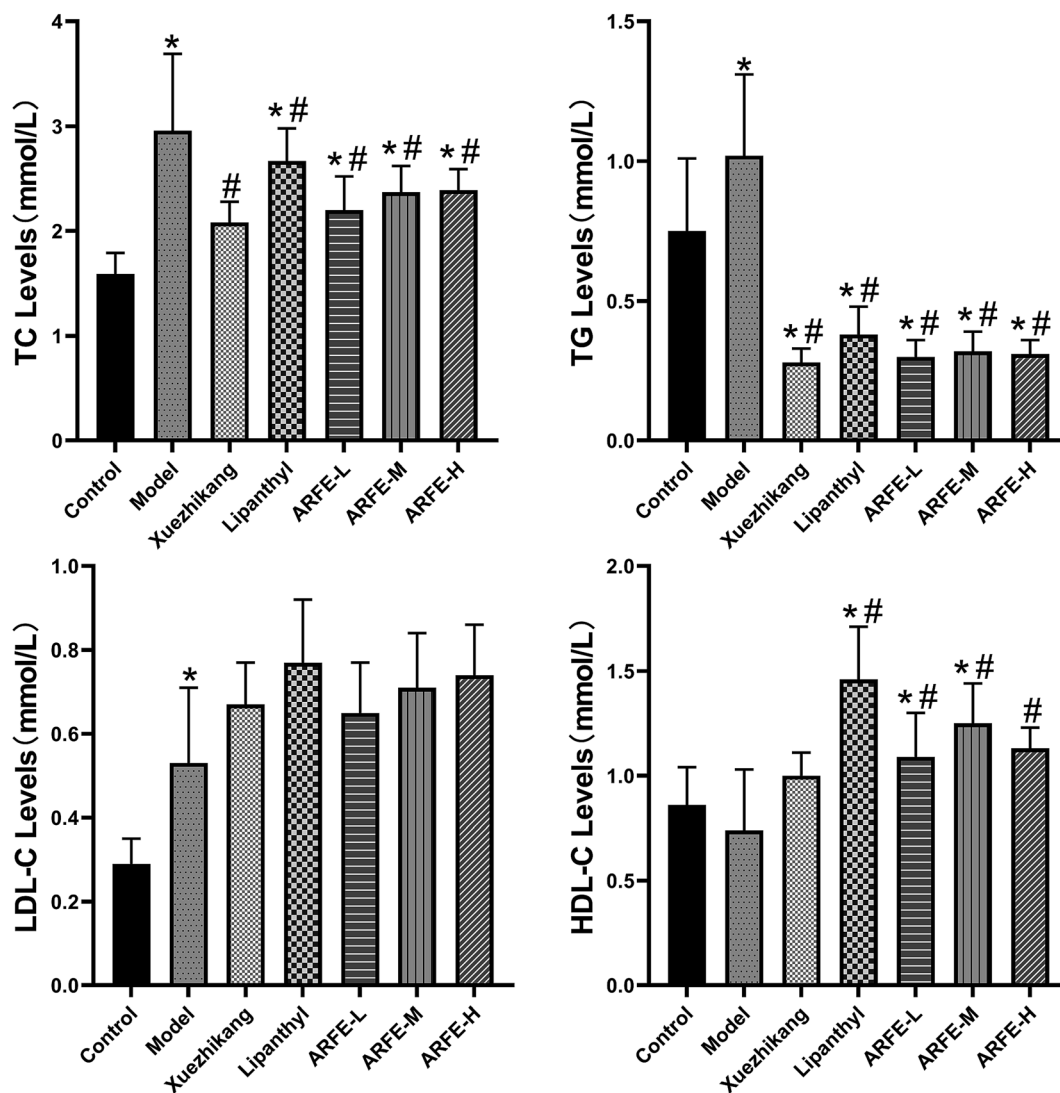


Fig. 4 Effect of ARFE on serum lipid levels in rats.  $P < 0.05$  indicates significant difference between two groups. \*, compare with Control group, #, compare with Model group.

### 3. Results

#### 3.1 HPLC analysis

The contents of apiin, 3'-methoxyapiin and apigenin-7-O- $\beta$ -D-glucopyranoside in D101 resin-purified dry solids were 18.73%, 4.85% and 1.24% respectively (Fig. 2 and Table 1). HPLC method validation is shown in Table 2, which indicates its reliability for measuring ARFE concentration. The quality control data of the three batches of ARFE extracts are shown in Table 3.

#### 3.2 Effects of ARFE on weight and liver index

As shown in Table 4, the body weight of the modeled rats was significantly higher compared to the controls ( $P < 0.05$ ) during the HLP induction period, and decreased significantly during the treatment regimen from week 6 to 11 (all  $P < 0.05$  compared to untreated model group). In addition, the HLP rats had

significantly higher liver index compared to the controls ( $P < 0.05$ ) due to excessive fat consumption (Fig. 3). In contrast, the liver index was significantly lower in each treatment group compared to the untreated model group ( $P < 0.05$ ), indicating that both the reference drugs and ARFE can inhibit the development of fatty liver. Furthermore, ARFE increased liver index relative to the control, indicating that it did not cause liver damage in the rats.

#### 3.3 Serum TC, TG, HDL-C and LDL-C analysis

Serum samples were analysed using an automated biochemical analyser (Fig. 4). Compared to the untreated HLP rats, the ARFE-treated animals had significantly reduced serum TC and TG levels and increased serum HDL-C levels (all  $P < 0.05$ ). However, the LDL-C levels were unaffected by ARFE.



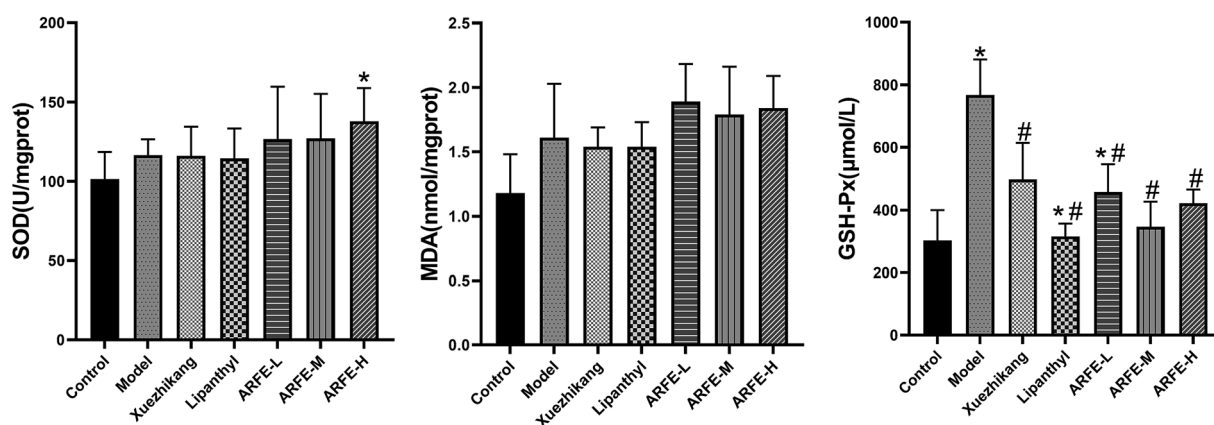


Fig. 5 Effect of ARFE on oxidative stress-associated factors in the liver of rats.  $P < 0.05$  indicates significant difference between two groups. \*, compare with Control group, #, compare with Model group.

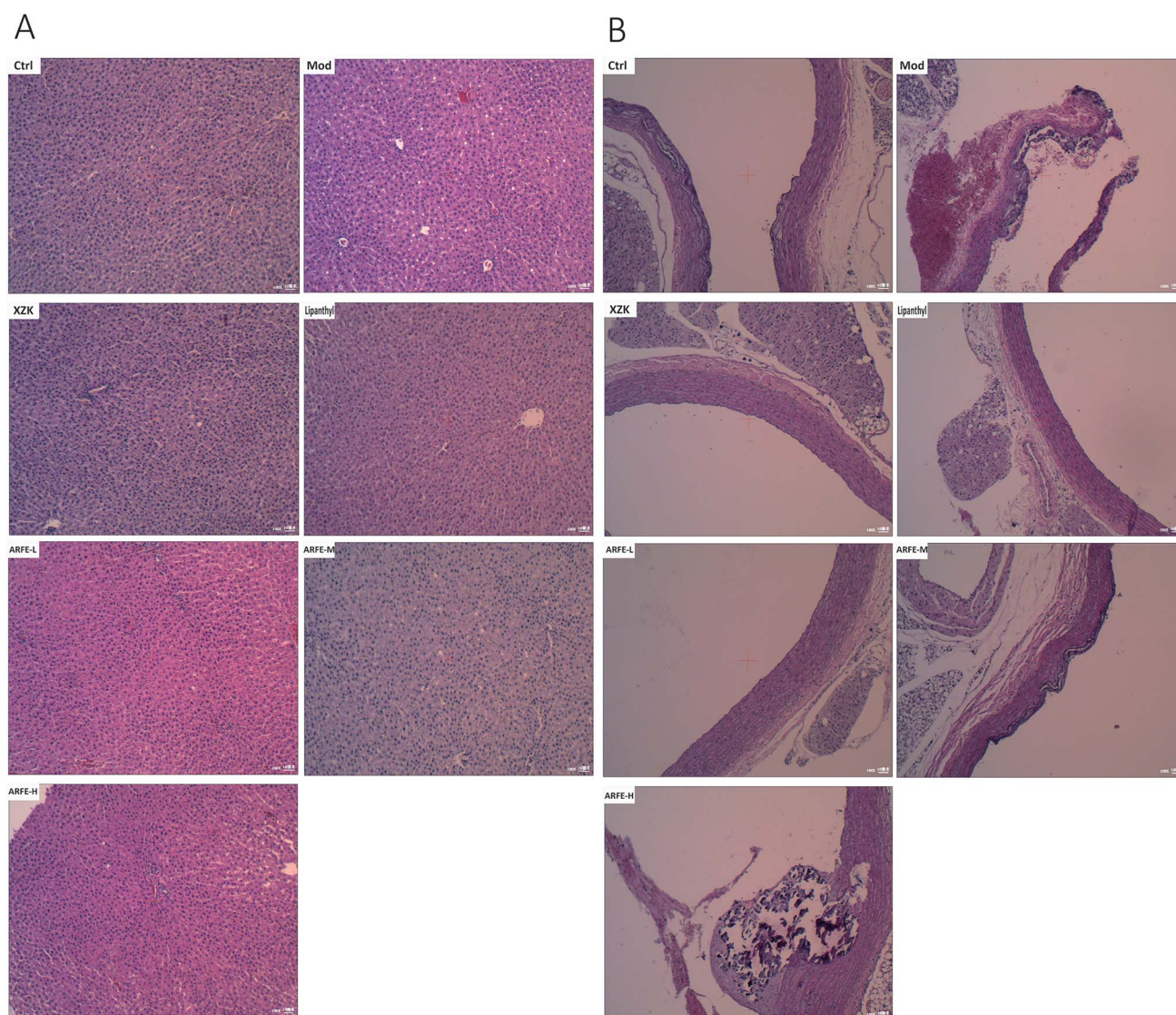


Fig. 6 Histopathological changes in the liver (A) and aortic arch (B) (H&E staining, 100 $\times$ ).

Table 5 Building pocket parameters

Order	Name of receptor	Center_x	Center_y	Center_z	Size_x	Size_y	Size_z
1	Acetyl-CoA carboxylase	30	1	5	104	86	126
2	AMP-dependent protein kinase	-19	35	-9	78	96	72
3	Adiponectin	1	-27	-1	44	50	52
4	Sterol regulatory element-binding protein 1	28	22	154	90	118	122
5	HMG-CoA reductase	9	-12	15	78	102	102
6	Squalene synthase	-27	50	45	76	90	80
7	Bile acid receptor	4	21	45	30	46	54
8	HMG-CoA synthetase	31	69	8	70	66	64
9	Farnesyl pyrophosphate synthase	8	29	38	66	78	58
10	NPC1L1	-14	-24	-12	36	60	46
11	LFA-1	54	28	35	52	66	54
12	Human apolipoprotein C-II	102	-2	1	34	38	32
13	Diacylglycerol acyltransferase 1	-5	-9	4	22	28	26
14	Diacylglycerol acyltransferase 2	31	41	18	54	42	46

### 3.4 Liver SOD, MDA and GSH-Px analysis

A previous study showed that HLP pathogenesis is associated with oxidative stress and lipid peroxidation.<sup>27</sup> Tissue MDA and GSH-Px levels and SOD activity are indices of oxidative stress and lipid peroxidation, as well as of free radical clearance and antioxidant capacity.<sup>28-31</sup> Compared to the untreated HLP rats

(Fig. 5), ARFE-H rats have significantly higher SOD activity ( $P < 0.05$ ), and lower GSH-Px levels ( $P < 0.05$ ). However, the liver MDA level was unaffected by ARFE treatment.

Table 6 Molecular docking results (ordered by increasing binding energy)

Number	Binding energy (kcal mol <sup>-1</sup> )	Number	Binding energy (kcal mol <sup>-1</sup> )
C-8	-11	A-9	-8.7
C-1	-10.9	B-2	-8.7
A-4	-10.5	B-4	-8.7
D-1	-10.5	B-9	-8.7
A-1	-10.4	C-14	-8.7
C-4	-10.4	B-6	-8.5
D-4	-10.4	B-10	-8.4
A-6	-10.2	C-11	-8.4
B-8	-10.1	A-8	-8.3
C-9	-10.1	C-3	-8.3
D-6	-10	D-8	-8.3
C-5	-9.6	A-11	-8.1
B-7	-9.5	B-5	-8.1
A-5	-9.4	D-11	-8
C-7	-9.4	D-12	-7.9
B-1	-9.3	A-10	-7.8
D-5	-9.3	B-3	-7.8
D-7	-9.2	B-14	-7.8
D-9	-9.2	D-10	-7.8
A-7	-9.1	B-11	-7.7
C-6	-9.1	A-12	-7.6
D-2	-9.1	C-12	-7.5
D-14	-9.1	C-10	-7.2
A-2	-8.9	B-12	-7
A-3	-8.9	C-13	-6.8
A-14	-8.9	D-13	-6.5
C-2	-8.8	A-13	-6.3
D-3	-8.8	B-13	-5.7

### 3.5 ARFE restores the HFD-induced histopathological changes in the liver and aortic arch

The high-fat emulsion-induced HLP significantly altered the structure of the liver and aortic arch (Fig. 6). While the liver of the control rats had no lesions, a distinct lobular structure, neatly arranged hepatic cords, radially organized hepatocytes around the central vein and only a few fat vacuoles, the HLP liver showed diffuse steatosis, disorganized hepatocytes, fat vacuoles and unclear lobular outline. ARFE treatment reduced the level of hepatic steatosis and significantly prevented liver damage (Fig. 6A). The aortic arch of control rats also showed no lesions, and had normal vascular structure and neatly arranged vascular cells. However, HLP resulted in a diffuse bulging in the vascular wall, accumulation of foam cells in the intima, and mineral deposition and necrotic plaques in the blood vessels. The ARFE-treated rats on the other hand had smoother vascular walls, reduced foam cell accumulation, and decreased mineral deposition and necrotic plaques (Fig. 6B). Therefore, ARFE can prevent fatty liver disease and atherosclerosis.

### 3.6 Identification of potential ARFE receptors by molecular docking

The HLP-associated receptor proteins identified by database and literature search included acetyl-CoA carboxylase (1), AMP-dependent protein kinase (2), adiponectin (3), sterol regulatory element-binding protein 1 (4), HMG-CoA reductase (5), squalene synthase (6), bile acid receptor (7), HMG-CoA synthetase (8), farnesyl pyrophosphate synthase (9), NPC1L1 (10), LFA-1 (11), human apolipoprotein C-II (12), diacylglycerol acyltransferase 1 (13), and diacylglycerol acyltransferase 2 (14). They were sequentially docked by apigenin (A), apiin (B), 3'-methoxy-yapiin (C), and apigenin-7-O-β-D-glucopyranoside (D). The results were arranged in the order of decreasing binding energy

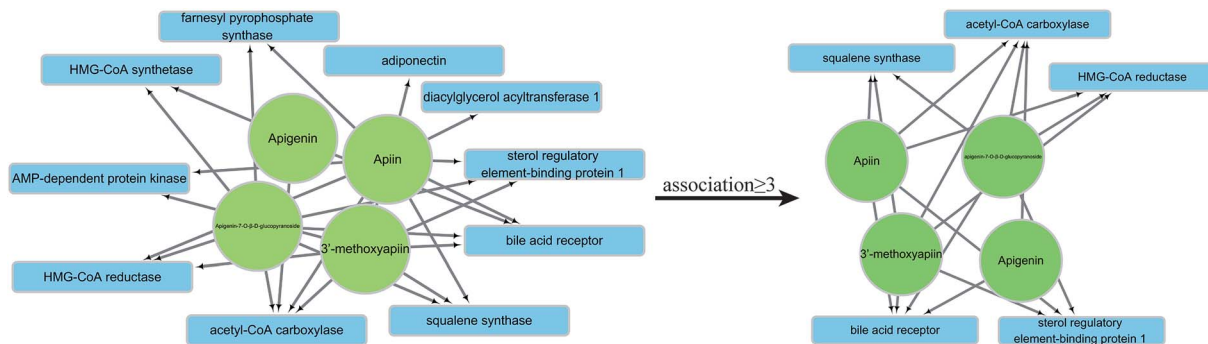


Fig. 7 Neural network and selection process.

(Table 6), and a neural network was constructed. Receptors with  $\geq 3$  association were selected for further analysis (Fig. 7).

### 3.7 Validation of ARFE receptors

FDFT1, SREBP1, HMGCR and ACC1 are the key enzymes in HLP development. Compared to the untreated modelled animals, the ARFE-treated rats had significantly reduced SREBP1 and HMGCR levels (both  $P < 0.05$ ), along with slightly lower ACC1 and higher FDFT1 levels (Fig. 8). These results indicated that the lipid-lowering effect of ARFE is mediated *via* the inhibition of SREBP1, HMGCR and ACC1.

### 3.8 Combination analysis of ARFE binding to SREBP1, HMGCR and ACC1

Validated results from western blotting were visualized using PyMOL and LigPlot+ v2.1.<sup>32</sup> We found multiple 3.5 Å hydrogen bonds when apigenin, apiin, 3'-methoxyapiin and apigenin-7-O- $\beta$ -D-glucopyranoside were each bound to SREBP1, HMGCR or ACC1. Spatial conformation of the ligands and receptors revealed that the ligands can effectively bind to the cavity of the receptors (Fig. 9).

## 4. Discussion

We selected fenofibrate and Xuezhikang as the positive reference drugs for this study. Previous studies have reported that long-term clinical use of fenofibrate can result in liver and muscle toxicity.<sup>33–35</sup> Red yeast is the main ingredient of Xuezhikang capsule, and its lipid-lowering effect is attributed to the presence of lovastatin,<sup>36</sup> which can cause side effects like thrombocytopenia<sup>37</sup> and diabetes.<sup>38</sup> ARFE contains multiple ingredients that act synergistically to treat HLP without any reported side effects. To examine the lipid-lowering and antioxidant effects of ARFE, we established a rat model of high-fat emulsion diet-induced HLP, and treated the rats with low ( $90 \text{ mg kg}^{-1}$ ), medium ( $180 \text{ mg kg}^{-1}$ ) or high ( $270 \text{ mg kg}^{-1}$ ) dose of ARFE. Surprisingly, ARFE did not decrease the serum lipid levels in a dose-dependent manner, which is likely due to the complexity of herbal medicine extracts, and the presence of various active components that exert their effects through multiple pathways and targets. Even if a medicinal formulation has only one target organ, multiple cellular and molecular targets may be involved. Furthermore, the extract may have a simultaneous reflective action on another target organ, and

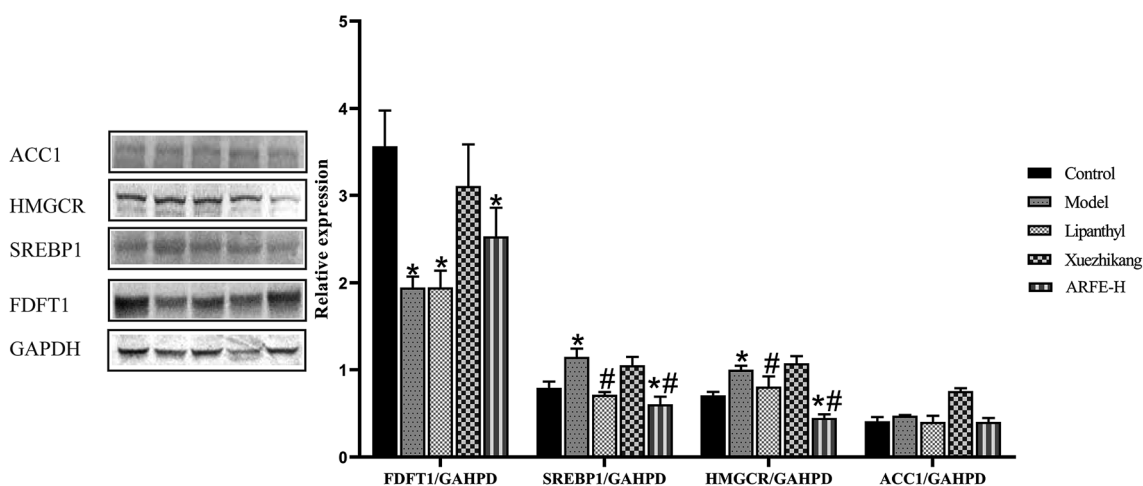


Fig. 8 FDFT1, SREBP1, HMGCR and ACC1 protein status and gene expression.  $P < 0.05$  indicates significant difference between two groups. \*, compare with Control group, #, compare with Model group.



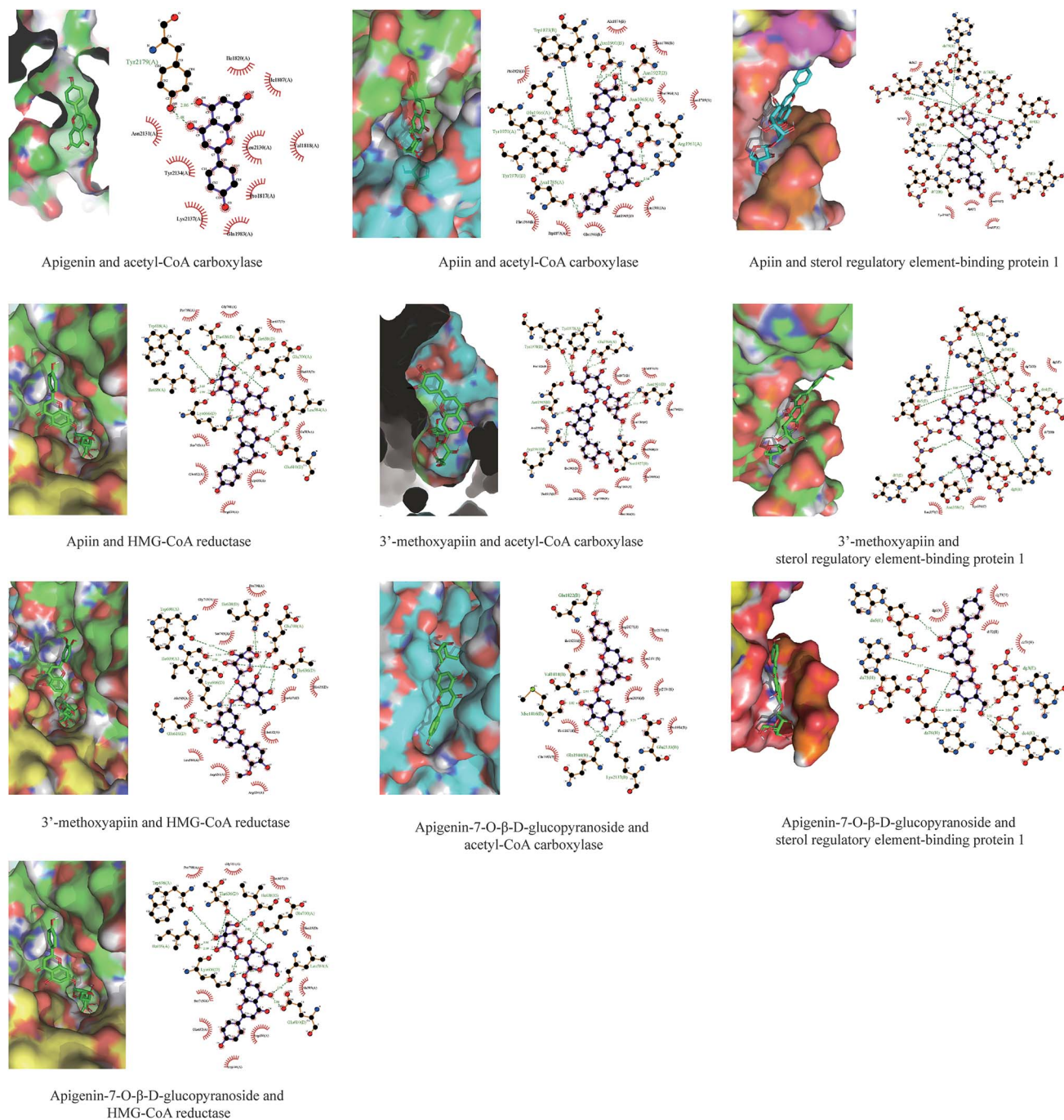


Fig. 9 Mode of ARFE binding to SREBP1, HMGCR and ACC1.

different receptors of the same drug component may have different thresholds. The lack of dose responsiveness seen in our study can also be explained by an upper limit of the transport rate of the effective components. In addition, the purified ARFE extract prepared in this study still included other non-flavonoid components, which may also affect the pharmacodynamic effect and absorption and transportation effect of the effective components. According to published literature,<sup>39,40</sup> GSH-Px activity in the liver is inversely proportional to the degree of liver fibrosis. In the early stage of non-alcoholic fatty

liver disease (NAFLD), the liver has only mild inflammation without liver fibrosis, which triggers production of GSH-Px that suppresses oxidative stress. Therefore, GSH-Px activity is generally higher in NAFLD patients than in healthy individuals. ARFE did increase the SOD activity and lower GSH-Px activity in liver tissues, indicating that it can effectively improve the pathological changes in the liver of HLP rats by reducing the oxidative stress level. However, the exact mechanism is still unclear and needs to be further investigated. Apigenin was previously reported to have an anti-HLP function.<sup>41,42</sup> Although

we did not detect apigenin among the chemical components of ARFE in our previous study, the ARFE-treated rats in this study had apigenin in their plasma. This could be the result of deglycosylation of apiin, 3'-methoxyapiin and apigenin-7-O- $\beta$ -D-glucopyranoside in the liver-gut circulation, which results in the generation of apigenin as a metabolite. This is consistent with the findings of Williamson *et al.*, wherein after the absorption of dietary flavonoids, some glycosides are de-glycosylated in the liver-gut circulation and absorbed as aglycones.<sup>43</sup> Therefore, we examined the probability of apigenin binding as a ligand to lipid-lowering targets using molecular docking.

Natural herbal medicines have multiple active ingredients and targets, and low active ingredient content, all of which are unfavourable for mechanistic studies. However, molecular docking is useful for analysing the multi-ingredient and multi-target properties of herbal medicines. We conducted database search and literature review to identify HLP-associated receptors, and then performed molecular docking with the three chemical ingredients of ARFE and a metabolite. Based on the results, the receptors that met the screening criteria were subjected to further validation. This method has the advantages of requiring fewer reagents and time compared to routine screening methods. Chen *et al.*<sup>44</sup> recommended that computer analysis results must be validated by biochemical assays on small samples. Therefore, we validated the selected receptors (FDFT1, ACC1, SREBP1 and HMGCR) through western blotting, and found that ARFE inhibited SREBP1, HMGCR and ACC1. SREBP1 is a cholesterol sensor localized to the endoplasmic reticulum which regulates intracellular cholesterol levels in a feedback manner *via* the Insig-Srebp-Scap pathway. HMGCR is the rate-limiting enzyme of the mevalonate pathway, which produces cholesterol and other isoprenoids. ACC1 is a biotinidase that converts acetyl-CoA to malonyl-CoA, which controls the rate of the first stage of fatty acid synthesis. Taken together, our results showed that the therapeutic effect of ARFE in HLP is mediated by the synergistic action of apigenin, apiin, 3'-methoxyapiin and apigenin-7-O- $\beta$ -D-glucopyranoside on SREBP1, HMGCR and ACC1. Our subsequent study will focus on elucidating the complete molecular mechanism.

## 5. Conclusions

ARFE has lipid-lowering and antioxidant properties, and the former is mediated by the inhibition of SREBP1, HMGCR and ACC1 expression. Therefore, ARFE is a promising drug for HLP treatment.

## Conflicts of interest

The authors declare no competing financial interest.

## Acknowledgements

This work received supported from National Natural Science Foundation of China (81460590).

## References

- 1 A. M. Navar-Boggan, E. D. Peterson, R. B. D'Agostino, B. Neely, A. D. Sniderman and M. J. Pencina, *Circulation*, 2015, **131**, 451–458.
- 2 R. H. Nelson, *Prim. Care*, 2013, **40**, 195–211.
- 3 R. A. Carr, B. J. Rejowski, G. A. Cote, H. A. Pitt and N. J. Zyromski, *Pancreatolgy*, 2013, **16**, 469–476.
- 4 B. Li, C. Zhang and Y. T. Zhan, *Can. J. Gastroenterol. Hepatol.*, 2018, **2018**, 2784537.
- 5 F. Lammert, K. Gurusamy, C. W. Ko, J. F. Miquel, N. Méndez-Sánchez, P. Portincasa, K. J. van Erpecum, C. J. van Laarhoven and D. Q. Wang, *Nat. Rev. Dis. Primers*, 2016, **2**, 16024.
- 6 T. Wilcox, J. D. Newman, T. S. Maldonado, C. Rockman and J. S. Berger, *Atherosclerosis*, 2018, **275**, 419–425.
- 7 S. Chen, X. Guo, S. Dong, S. Yu, Y. Chen, N. Zhang and Y. Sun, *Clin. Rheumatol.*, 2017, **36**, 1111–1119.
- 8 B. Bozkurt, D. Aguilar, A. Deswal, S. B. Dunbar, G. S. Francis, T. Horwich, M. Jessup, M. Kosiborod, A. M. Pritchett, K. Ramasubbu, C. Rosendorff and C. Yancy, *Circulation*, 2016, **134**, e535–e578.
- 9 C. Ricci, M. Gaeta, E. Rausa, E. Asti, F. Bandera and L. Bonavina, *Obes. Surg.*, 2015, **25**, 397–405.
- 10 T. Sugai, Y. Suzuki, M. Yamazaki, K. Shimoda, T. Mori, Y. Ozeki, H. Matsuda, N. Sugawara, N. Yasui-Furukori, Y. Minami, K. Okamoto, T. Sagae and T. Someya, *PLoS One*, 2016, **11**, e0166429.
- 11 N. Katsiki, D. P. Mikhailidis and C. S. Mantzoros, *Metab., Clin. Exp.*, 2016, **65**, 1109–1123.
- 12 M. Bahmani, M. Mirhoseini, H. Shirzad, M. Sedighi, N. Shahinfard and M. Rafeian-Kopaei, *J. Evidence-Based Complementary Altern. Med.*, 2015, **20**, 228–238.
- 13 J. Kolarovic, M. Popovic, J. Zlinská, S. Trivic and M. Vojnovic, *Molecules*, 2010, **15**, 6193–6204.
- 14 M. K. Gharib Naseri, A. A. Pilehvaran and N. Shamansouri, *Feyz*, 2007, **11**, 1–7.
- 15 W. Kooti, M. Ghasemiboroon, M. Asadi-Samani, A. Ahangarpour, M. Noori Ahmad Abadi, R. Afrisham and N. Dashti, *Adv. Environ. Biol.*, 2014, **8**, 325–330.
- 16 K. Mansi, A. M. Abushoffa, A. Disi and T. Aburjai, *Pharmacogn. Mag.*, 2009, **5**, 301.
- 17 A. Sipailiene, P. Venskutonis, A. Sarkinas and V. Cypiene, *Acta Hort.*, 2003, 71–77.
- 18 I. H. Sellami, I. Bettaieb, S. Bourgou, R. Dahmani, F. Limam and B. Marzouk, *J. Essent. Oil Res.*, 2012, **24**, 513–521.
- 19 N. Nikolić, D. Cvetković and Z. Todorović, *Ital. J. Food Sci.*, 2011, **23**, 214–221.
- 20 O. Trott and A. J. Olson, *J. Comput. Chem.*, 2010, **31**, 455–461.
- 21 F. Shao, L. Gu, H. Chen, R. Liu, H. Huang and G. Ren, *Pharmacogn. Mag.*, 2016, **12**, 64–69.
- 22 Y. H. Li, C. Y. Yu, X. X. Li, P. Zhang, J. Tang, Q. Yang, T. Fu, X. Zhang, X. Cui, G. Tu, Y. Zhang, S. Li, F. Yang, Q. Sun, C. Qin, X. Zeng, Z. Chen, Y. Z. Chen and F. Zhu, *Nucleic Acids Res.*, 2018, **46**, D1121–D1127.

- 23 X. Q. Nie, H. H. Chen, J. Y. Zhang, Y. J. Zhang, J. W. Yang, H. J. Pan, W. X. Song, F. Murad, Y. Q. He and K. Bian, *Acta Pharmacol. Sin.*, 2016, **37**, 483–496.
- 24 Z.-G. Zheng, C. Lu, P. M. Thu, X. Zhang, H.-J. Li, P. Li and X. Xu, *RSC Adv.*, 2017, **8**, 354–366.
- 25 J. Zhong, W. Gong, L. Lu, J. Chen, Z. Lu, H. Li, W. Liu, Y. Liu, M. Wang, R. Hu, H. Long and L. Wei, *Int. Immunopharmacol.*, 2017, **42**, 176–184.
- 26 J. Kang, C. Guo, R. Thome, N. Yang, Y. Zhang, X. Li and X. Cao, *RSC Adv.*, 2018, **8**, 30539–30549.
- 27 J. Bai, S. Zheng, D. Jiang, T. Han, Y. Li, Y. Zhang, W. Liu, Y. Cao and Y. Hu, *Int. J. Clin. Exp. Pathol.*, 2015, **8**, 13193–13200.
- 28 H. Zhang, M. Yin, L. Huang, J. Wang, L. Gong, J. Liu and B. Sun, *J. Food Sci.*, 2017, **82**, 278–288.
- 29 O. Ighodaro and O. Akinloye, *Alexandria Journal of Medicine*, 2018, **54**, 287–293.
- 30 L. Yuan and N. Kaplowitz, *Mol. Aspects Med.*, 2009, **30**, 29–41.
- 31 W. Samy and M. A. Hassanian, *Arab J. Gastroenterol.*, 2011, **12**, 80–85.
- 32 R. A. Laskowski and M. B. Swindells, *J. Chem. Inf. Model.*, 2011, **51**, 2778–2786.
- 33 N. Tarantino, F. Santoro, M. Correale, L. De Gennaro, S. Romano, M. Di Biase and N. D. Brunetti, *Drugs*, 2018, **78**, 1289–1296.
- 34 A. E. Power, L. V. Graudins, C. A. McLean and I. Hopper, *Am. J. Health-Syst. Pharm.*, 2015, **72**, 2061–2063.
- 35 S. Kim, K. Ko, S. Park, D. R. Lee and J. Lee, *Korean J. Fam. Med.*, 2017, **38**, 192–198.
- 36 J. Ying, L.-D. Du and G.-H. Du, in *Natural Small Molecule Drugs from Plants*, Springer, 2018, pp. 93–99.
- 37 Q. Zhao, M. Li, M. Chen, L. Zhou, L. Zhao, R. Hu, R. Yan and K. Dai, *Environ. Toxicol. Pharmacol.*, 2016, **42**, 69–75.
- 38 N. Sattar, D. Preiss, H. M. Murray, P. Welsh, B. M. Buckley, A. J. de Craen, S. R. Seshasai, J. J. McMurray, D. J. Freeman, J. W. Jukema, P. W. Macfarlane, C. J. Packard, D. J. Stott, R. G. Westendorp, J. Shepherd, B. R. Davis, S. L. Pressel, R. Marchioli, R. M. Marfisi, A. P. Maggioni, L. Tavazzi, G. Tognoni, J. Kjekshus, T. R. Pedersen, T. J. Cook, A. M. Gotto, M. B. Clearfield, J. R. Downs, H. Nakamura, Y. Ohashi, K. Mizuno, K. K. Ray and I. Ford, *Lancet*, 2010, **375**, 735–742.
- 39 G. Perlemuter, A. Davit-Spraul, C. Cosson, M. Conti, A. Bigorgne, V. Paradis, M. P. Corre, L. Prat, V. Kuocho, A. Basdevant, G. Pelletier, J. M. Oppert and C. Buffet, *Liver Int.*, 2005, **25**, 946–953.
- 40 X. B. Cai and L. G. Lu, *World Chin. J. Digestol.*, 2009, **17**, 3279–3282.
- 41 H. J. Liu, Y. L. Fan, H. H. Liao, Y. Liu, S. Chen, Z. G. Ma, N. Zhang, Z. Yang, W. Deng and Q. Z. Tang, *Mol. Cell. Biochem.*, 2017, **428**, 9–21.
- 42 K. Zhang, W. Song, D. Li and X. Jin, *Exp. Ther. Med.*, 2017, **13**, 1719–1724.
- 43 G. Williamson, C. D. Kay and A. Crozier, *Compr. Rev. Food Sci. Food Saf.*, 2018, **17**, 1054–1112.
- 44 Y. C. Chen, *Trends Pharmacol. Sci.*, 2015, **36**, 78–95.